SOLUTE ACCESSIBILITY TO N^{ϵ}-FLUORESCEIN ISOTHIOCYANATE-LYSINE-23 COBRA α-TOXIN BOUND TO THE ACETYLCHOLINE RECEPTOR

A Consideration of the Effect of Rotational Diffusion and Orientation Constraints on Fluorescence Quenching

DAVID A. JOHNSON* AND JUAN YGUERABIDE‡
*Division of Biomedical Sciences, University of California, Riverside, California 92521-0121; and
‡Department of Biology, University of California, San Diego, La Jolla, California 92093

ABSTRACT To obtain information on the disposition of α-toxin when bound to the acetylcholine receptor (AChR), we evaluated the accessibility of solutes to fluorescein isothiocyanate (FITC) conjugated to α-toxin (*siamensis* 3) at lysine 23 (FITC-toxin) by measuring the rate constants for iodide quenching of the fluorescence of fluorescein free in solution and FITC-toxin free in solution and bound to AChR. Relative to the free fluorescein, we observed a 55% reduction in the quenching rate constant for the unbound FITC-toxin and 80% reduction for the AChR-bound FITC-toxin. It is tempting to interpret a decrease in the quenching rate constant as due to an increase in the masking of the labeling fluorophore, which in our case would then be indicative of masking of fluorescein conjugated to the free toxin and masking of FITC-toxin, in the region of lysine 23, when bound to AChR. However, elementary considerations indicate that the quenching rate depends not only on geometrical masking factors but also on the translational and rotational mobilities of the labeled molecules as well as orientational constraints. To evaluate these effects we have established quantitative relations between the rate of fluorescence quenching, the degree of masking of fluorophore, translational and rotational rates, and orientational constraints of the labeled macromolecules, using recent formulations for the rate of reaction between asymmetric molecules (Shoup et al., 1981, *Biophys. J.*, 36:619–714). These relations predict that the decrease in quenching constant observed for the labeled FITC-toxin as well as the AChR-bound FITC-toxin is largely due to differences in translational and rotational rates and orientational constraints and not to significant increases in geometrical masking. Our theoretical formulation shows that the quenching rate can be decreased by a factor of 2–5 merely by immobilizing a fluorophore on the surface of a large protein without any significant increase in geometrical masking.

INTRODUCTION

Solute accessibility to fluorescent probes or groups attached to protein molecules is often used to monitor conformational aspects of these macromolecules. Solute accessibility is most often determined with fluorescence quenchers such as acrylamide and iodide by measuring and comparing the specific rate of quenching of the fluorophore free in solution, k_{FQ}, with its rate attached to the macromolecule, k_{MQ}, or by comparing values of k_{MQ} for two or more conditions that may affect the conformation of the protein. It is usually assumed that a decrease in quenching rate for the bound fluorophore indicates a decreased accessibility due to geometrical masking factors in the macromolecule. However, elementary considerations indicate that for the rapid, diffusion-limited reactions that characterize fluorescence quenching process, k_{MQ} should depend not only on masking factors but also on the translational and rotational mobilities of the labeled macromolecules as well as on orientational constraints imposed by the association of fluorophores with macromolecules. The lower the rotational mobility, the lower is the probability that a bound fluorophore, exposed on a small fraction of the surface area of the macromolecule, will meet a quencher molecule during its excited state lifetime. These notions are indeed supported by recent theoretical formulations on the reactivity of specific groups attached to macromolecules (Sloc and Stockmaker, 1971, 1973; Schmitz and Schurr, 1972; Schurr and Schmitz, 1976; Shoup et al., 1981).

In this paper we establish quantitative relations between

Please send correspondence to David A. Johnson, Division of Biomedical Sciences, University of California, Riverside, CA 92521-0121

the specific rate of quenching, k_{MQ}, translational and rotational mobilities, orientational constraints, and geometrical masking factors, using formulations of Shoup et al. (1981). We then use these relations to analyze iodide quenching data (steady state and time-resolved), which we have measured for (*a*) fluorescein free in solution and for fluorescein-labeled α-toxin (labeled at lysine 23); (*b*) free in solution; and (*c*) bound to the *Torpedo californica* acetylcholine receptor (AChR). The results give information on the extent to which the surface of the α-toxin molecule, in the region of lysine 23, is masked when bound to the AChR.

THEORY

In the fluorescence quenching experiment, the fluorescence intensities of the fluorophore attached to a macromolecule or free in solution are monitored as a function of the quencher concentration. The intensities are then analyzed with the Stern-Volmer equation

$$I_o/I = 1 + K_Q[Q], \quad (1)$$

where I_o and I are fluorescence intensities observed in the absence and presence of a concentration [Q] of quencher. K_Q, the quenching constant, is related to the bimolecular reaction rate, k_{FQ}, by the equation

$$K_Q = k_{FQ}\tau, \quad (2)$$

where τ is the fluorescence lifetime. The fundamental parameter for evaluating accessibility is k_{FQ}.

Quenching of Free Fluorophore in Solution

Quenching rate is determined by the rate of encounter between quencher and fluorescent molecule and the probability of reaction per encounter. For the case where the fluorophore, F, and quencher, Q, are spherical molecules, the encounter rate is given by the Fick equation

$$S = 4\pi R_{FQ}^2 D_{FQ} \partial n_Q(R,t)/\partial R (\text{molecule/s}), \quad (\text{at } R = R_{FQ}), \quad (3)$$

where D_{FQ} is the sum of the translational diffusion coefficients of F and Q. $n_Q(R, t)$ is the average concentration of quencher molecules at a distance R from an excited fluorophore molecule. R_{FQ} is the sum of the molecular radii of F and Q, R_F and R_Q, respectively. The partial derivative is the concentration gradient of quencher molecules about an excited F molecule evaluated at the distance $R = R_{FQ}$. S is essentially the flux due to translational diffusion of quencher molecules across a spherical surface of radius R_{FQ} surrounding an excited molecule and is just the rate of new encounters between F and Q. S is related to k_Q by the equation

$$k_Q = S/n_Q^\circ \ (\text{cm}^3/\text{molecule-s}), \quad (4)$$

where n_Q° is the concentration of quencher molecules in the bulk solution. According to theory (Yguerabide et al., 1964; Yguerabide, 1967), when an ensemble of excited molecules is first created by a pulse of light, the quenching rate is initially very high due to encounters between the F and Q molecules that happen to be in close proximity at the time of excitation. However, within 10^{-10} to 10^{-11} s, the system moves to a steady state with a gradient of quencher molecules around each fluorescent molecule. For the case where quenching occurs on every encounter, the specific quenching rate is then given by the Smoluchowski equation (Eq. 5).

$$k_{FQ} = 4\pi D_{FQ} R_{FQ}. \quad (5)$$

The interaction of quencher molecules with an excited fluorophore molecule attached to a macromolecule can be considered as an asymmetric reaction in which each quencher molecule behaves as a uniformly reactive sphere interacting with a macromolecular sphere that is reactive only on a limited portion of its surface area as shown in Fig. 1. The reactive area is characterized by the cone angle $2\theta_o$ shown in the figure. For such a reaction, the rate constant depends not only on the collision frequency between quencher and spherical macromolecule (determined by radii and translational diffusion coefficients as shown by the Smoluchowski equation) but also on the rotational mobility of the macromolecule and θ_o. This is because the number of encounters between a macromolecule and its surrounding quencher molecules, that are effective at the reactive area, depends on the rotational mobility of the macromolecule. Various authors have offered approximate solutions for this type of reaction, based on considerations of the combined translational and rotational diffusion equations. Here, we follow the solution of Shoup et al. (1981) for the analogous reaction. Since the bimolecular reaction rate constant is the quenching rate constant, k_{MQ}, in the steady state, we can evaluate k_{MQ} by Eq. 6 (see Eq. 22 in Shoup et al., 1981).

$$k_{MQ} = \frac{8\pi D_{MQ} R_{MQ}^2 \kappa (1 - \cos\theta_o)^2}{4D_{MQ}(1 - \cos\theta_o) - \kappa R_{MQ} \sum_{n=0}^{\infty} \cdot \frac{[P_{n-1}(\cos\theta_o) - P_{n+1}(\cos\theta_o)]^2 K_{n+1/2}(\xi_n^*)}{(n + 1/2)\,[(nK_{n+1/2})(\xi_n^*) - \xi_n^* K_{n+3/2}(\xi_n^*)]}}, \quad (6)$$

where

$$\xi_n^* = R_{MQ}[n(n+1)D_R/D_{MQ}]^{1/2}. \quad (7)$$

$D_R(s^{-1})$ is the rotational diffusion coefficient of the macromolecule and κ is a parameter related to the probability of reaction upon encounter. κ approaches a value of infinity for a probability of 1. K is a parameter of a modified spherical Bessel function of the third kind and $P_n(\cos\theta_o)$ is the nth order Legendre polynomial (Abramowitz and Stegun, 1965).

We use the following procedure to compare our experimental fluorescence quenching data with calculated theoretical rates based on Eq. 6. According to this equation, the quenching rate constant for a fluorescently labeled macromolecule is determined by the values of D_M, D_R, R_M, D_Q, R_Q, and θ_o. For a spherical protein molecule, D_M, D_R, and D_Q can be

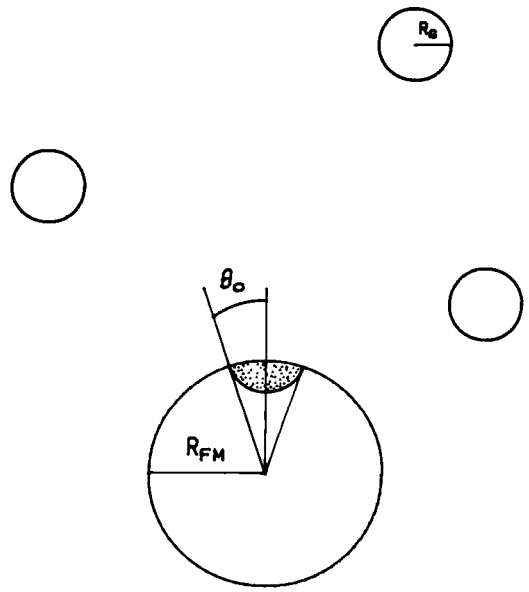

FIGURE 1 Model (based on Solc and Stockmaker, 1971 and 1973) for the interaction of a uniformly reactive quencher with a spherical macromolecule reactive only in an area circumscribed on its surface by a cone drawn from its center with cone angle of $2\theta_o$.

evaluated from the molecular weight of the protein with Eqs. 10–14 in the Appendix. Values for D_Q and R_Q can be obtained from the literature. The parameter θ_o, can be evaluated as follows. We assume that the fluorophore is treatable as a spherical particle of radius R_F and that the bound fluorophore occupies an area of $4\pi R_F^2$ on the surface of the macromolecule when the fluorophore is fully exposed (completely accessible). The fraction of the protein surface area, F^o_{FM}, occupied by the fully exposed fluorophore is then given by

$$F^o_{FM} = R_F^2/(R_M^2 + R_F^2). \quad (8)$$

For the case where the fluorophore is only partially exposed to the quencher, we let f_{MQ} represent the fraction of the fluorophore's surface-area, $4\pi R_F^2$, that is exposed on the surface of the macromolecule. f_{MQ} ranges from 0 to 1 for the completely nonexposed to completely exposed fluorophore and is a measure of quencher accessibility. The fraction of protein surface area occupied by the partially exposed fluorophore is then given by

$$F_{FM} = [f_{MQ}R_F^2/(R_M^2 + f_{MQ}R_F^2)]. \quad (9)$$

F_{FM} can thus be evaluated by assigning a value to f_{MQ} and using the values for R_M and R_F obtained as described in the Appendix. Finally, θ_o can be evaluated with the known equation for the fraction of a sphere's surface area circumscribed by θ_o,

$$\cos\theta_o = 1 - 2F_{FM}. \quad (10)$$

With the procedure described above, we have evaluated k_{MQ} for proteins of different molecular weight and different values of f_{MQ} assuming a very large value for κ as is expected for rapid quenching processes that occur in the nanosecond time range. k_{MQ}, the quenching rate constant for the free fluorophore, was calculated with Eq. 5 using $D_F = 4.3 \times 10^{-6}$ cm^2/s and $R_F = 5.3$Å for fluorescein. Fig. 2 *A* shows a plot of k_{MQ}/k_{FQ} vs. molecular weight of protein for the fully exposed fluorophore ($f_{MQ} = 1$). Fig. 2 *B* shows plots of k_{MQ}/k_{FQ} vs. f_{MQ} for the partially exposed fluorophore and proteins with molecular weights of 8, 250, and 9,000 kilodaltons. Fig. 2 *A* essentially shows the effects on k_{MQ} of the limited translational and rotational mobility of the macromolecule compared with the free fluorophore whereas the plots of Fig. 2 *B* show the additional effects introduced by geometrical masking as measured by f_{MQ}. k_{MQ}/k_{FQ} decreases very rapidly until the mass of the protein reaches ~50 kilodaltons, after which it tends to bottom out at ~0.38 (Fig. 2 *A* and *B*). According to Fig. 2 *B*, the accessibility parameter, f_{MQ}, is not linearly related to the quenching constant, in particular for $f_{MQ} < 0.2$.

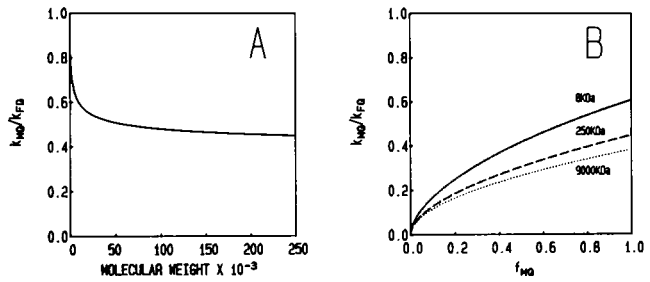

FIGURE 2 Theoretical plots based on Eq. 6 of the ratio of iodide ion quenching rate constants for fluorescein bound to a spherical protein (k_{MQ}) and fluorescein free in solution (k_{FQ}) vs. *A*, the molecular mass of the protein conjugate assuming total accessibility of iodide to the fluorophore and *B*, the fractional accessibility (f_{MQ}) of iodide to protein-conjugated fluorescein. The fluorophore is assumed to be spherical with a molecular mass of FITC ($M_r = 389$). The solid line in panel *B* assumes a molecular mass of the protein to be 8 kilodaltons, dashed line 250 kilodaltons, and dotted line 9,000 kilodaltons. The radius of the fluorophore was assumed to be 5.3 Å. The translation diffusion rate of fluorescein was estimated to be 4.3×10^{-6} cm$^2 \cdot$ s^{-1} utilizing Eq. 14. The radius and translational diffusion rate of the protein conjugates were estimated using eqs. 14 and 16, respectively.

Based on the above theoretical calculations, the conjugation of FITC to the cobra α-toxin (8 kilodaltons) should decrease the quenching rate constant, relative to the free fluorophore, by ~39%, while the binding of the labeled α-toxin to the membrane-associated acetylcholine receptor (≫250 kilodaltons) should further reduce the rate constant by ~38%, apart from possible masking effects.

EXPERIMENTAL PROCEDURES

Materials

Cobra α-toxin (*siamensis* 3) was isolated following the method of Karlsson et al. (1971) from *Naja naja siamensis* venom obtained lyophilized from Miami Serpentarium (Miami, FL). FITC-toxin was prepared as described elsewhere (Johnson and Taylor, 1982) and subsequently purified by column isoelectric focusing as described previously (Weiland et al., 1976). Analytical isoelectric focusing of this material indicated 98% homogeneity based on the distribution of fluorescence. Mono-[^{125}I] tyrosine 25 α-toxin (*siamensis* 3) was prepared and separated from noniodinated and diiodo species by column isoelectric focusing (Weiland *et al.*, 1976). All other reagents were at least reagent grade.

Receptor Isolation

Receptor-rich membrane fragments were isolated from *Torpedo californica* electric organ following published procedures (Johnson and Taylor, 1982: Reed et al., 1975). Aprotin (2.7 trypsin inhibitor units per 100 g tissue), phenylmethyl-sulfonylfluoride (0.9 mg per 100 g tissue), and EGTA (5 mM) were added during the initial homogenization to minimize proteolysis. The specific binding activities of the receptor preparations were measured by adsorption of mono[^{125}I] α-toxin-receptor complexes onto Whatman DE-81 (Clifton, NJ) filters (Schmidt and Raftery, 1975) and ranged between 1 and 2 nmol of α-toxin binding sites per mg protein. Incubation of 10-fold excess of native toxin 30 min prior to the addition of mono[^{125}I]α-toxin defined the 'nonspecific' binding component in the total binding.

Fluorescence Lifetime Analysis

Fluorescence lifetimes were determined by the single-photon counting technique using an EEY scientific nanosecond fluorometer (La Jolla, CA) equipped with a high-pressure hydrogen arc lamp. Data accumulated in a E.G. & G. Ortec 7150 multichannel analyzer (Salem, MA), were analyzed and displayed by using a Compaq computer (Houston, TX) and a Hewlett-Packard 7470A plotter (San Diego, CA). Excitation and emission bands were selected with an Oriel 5754 interference (Stamford, CT) and a Corning 3-68 cut-off filter (Corning, NY), respectively. Fluorescence decay rates were resolved and assessed as either single or double exponential functions by using the method of moments. The instrumental arrangement and principles of data treatment have been discussed in detail (Yguerabide, 1972; Yguerabide and Yguerabide, 1984).

The intensity, $I(t)$, vs. time graph, directly measured with the nanosecond fluorometer is distorted by the finite duration of the lamp pulse, $L(t)$, and is related to the nondistorted time course of emission $F(t)$ by the convolution integral (Eq. 11).

$$I(t) = \int_o^t L(T)F(t - T)dT. \quad (11)$$

$F(t)$ was obtained from measured graphs of $I(t)$ and $L(t)$ by deconvolution with the method of moments, assuming that $F(t)$ can be represented by a one- or two-exponential expression. The time shift between $L(t)$ and $I(t)$ introduced by the spectral response properties of the detecting

photomultiplier tube was corrected with a time shift introduced by the computer. Convolution of $F(t)$ so obtained with $L(T)$ generates a new function $C(t)$ that can be compared with $I(t)$. The values of coefficients and lifetimes are chosen so that the reduced chi square, χ^2_N/N, is a minimum.

$$\chi^2_N/N = 1/(N-n) = 1/(N-n)\,\Sigma\,(1/\sigma_i^2)[I(t_i) - C(t_i)]^2, \quad (12)$$

where σ_i is the standard deviation of $I(t_i)$ due to noise, N is the total number of data points and n is the number of parameters being fitted.

Fluorescence Titrations

All steady state fluorescence measurements were made on a Farrand Mark I spectrofluorometer (Valhalla, NY) equipped with corrected excitation and a Hamamatsu R928 photomultiplier tube (Middlesex, NJ). The spectrofluorometer was interfaced to a Tektronix 4052 microcomputer (Beaverton, OR) via a TransEra analog-to-digital converter (Provo, Utah). Samples were maintained at constant temperature in a four-position cell holder turret housed in a water jacketed sample compartment controlled with a Haake thermostat (Saddle Brook, NJ). Fluorescence titrations were carried out using 1 cm^2–cross-section cuvettes at 20°C. The samples were excited at 480 nm with a Farrand 480 filter in the path of the excitation beam. The emission was monitored at 519 nm with a Corning 3-70 filter in the path of the emission beam. Fluorescence values were corrected for dilution resulting from added titrant, lamp fluctuations, and light scatter. Unless indicated otherwise, all samples were dissolved in 0.1 M NaCl, 10 mM sodium phosphate buffer, pH 7.4, and 0.1 mM sodium thiosulfate to prevent formation of triiodide anion.

RESULTS

Nanosecond Lifetime Determinations

Fluorescence decay rates of FITC-toxin free in solution or bound to the acetylcholine receptor reasonably conformed to monoexponential behavior (Figs. 3 *A* and 3 *B*) and were calculated to be 3.9 and 3.8 ns, respectively.

Iodide Quenching

The Stern-Volmer plots for iodide quenching of the fluorescence of fluorescein, FITC-toxin in the presence of native α-toxin-saturated acetylcholine receptor, and FITC-toxin bound to the acetylcholine receptor are shown in Fig. 4. The slopes (K_Q's) of linear least squares fits to these plots are presented in Table I. Both Stern-Volmer quenching plots of FITC-toxin are linear to at least 0.6 M KI (all data not shown) but the fluorescein plot is only linear to ~0.12 M KI. Using Eq. 2 and the measured lifetimes, the quenching rate constants were calculated (Table I). The quenching rate constant of the fluorescein moiety decreased to 45% upon conjugation to the α-toxin and by 80% following binding of the conjugated α-toxin to the receptor.

To assess possible effects of the AChR-associated membranes, iodide quenching of the fluorescence of FITC-toxin in the absence of receptor was determined (data not shown). The Stern-Volmer plots of these titrations yielded quenching constants essentially identical with those observed for FITC-toxin in the presence of native α-toxin saturated receptor, indicating that the presence of the AChR-associated-membrane-induced turbidity did not affect the results.

To assess possible surface charge effects on the negatively charged iodide anion, we measured the quenching constants for samples in 1.0 M instead of 0.1 M NaCl (data not shown). We observed only a slight increase in the quenching rate constants, suggesting that the observed differences are not due to differences in surface charge.

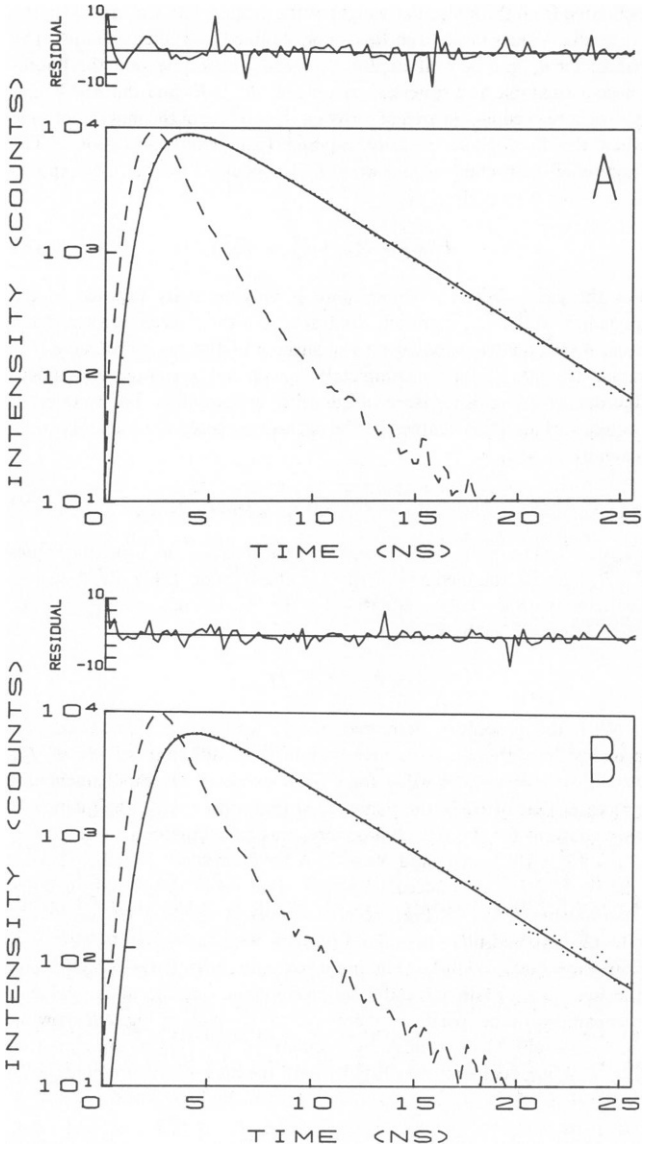

FIGURE 3 Nanosecond fluorescence decay curves (*A*) of FITC-toxin (500 nM) bound to the acetylcholine receptor (750 nM in α-toxin sites) and (*B*) of FITC-toxin (500 nM) free in solution in the presence of native α-toxin (4 μM) bound acetylcholine receptor α-toxin binding sites (750 nM in α-toxin sites). Dashed lines represent lamp pulse. Deviation of the experimental (dotted) from a single exponential theoretical (solid) function are shown in the upper curves. The χ^2_N/N for the deviation in the upper and lower panels are 1.9 and 1.8, respectively. Native α-toxin was incubated with the receptor 30 min prior to the addition of FITC-toxin. The FITC-toxin was then incubated an additional 45 min before the lifetimes were determined to insure that more than 95% of the FITC-toxin was bound.

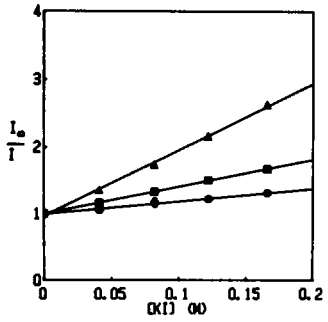

FIGURE 4 Stern-Volmer plots of iodide quenching of the fluorescence of fluorescein (triangles), FITC-toxin bound to the acetylcholine receptor (circles), and FITC-toxin free in a solution containing native α-toxin-saturated acetylcholine receptor (squares). Error bars ($n = 3$) are not shown when they fall within symbol. The concentrations of fluorescein, FITC-toxin, acetylcholine receptor and native-toxin were 50 nM, 122 nM, 300 nM (in α-toxin sites), 3 μM, respectively. Native α-toxin was incubated with the receptor for 30 min prior to the addition of FITC-toxin. This mixture was incubated an additional 45 min to insure that at least 95% of the FITC-toxin was bound to the AChR. Solid lines represent linear least squares fits to the data.

DISCUSSION

To obtain information on the disposition of cobra α-toxin bound to the surface of the AChR, we determined the solute accessibility to FITC conjugated to AChR-bound N^{ϵ}-lysine 23 α-toxin. We measured the Stern-Volmer iodide quenching constants and fluorescence lifetimes of the conjugated α-toxin free in solution and AChR-bound and of fluorescein free in solution. From the fluorescence lifetimes and quenching constants, we calculated the bimolecular quenching rate constants, which are the fundamental parameters for evaluating accessibility. The magnitudes of the quenching rate constants of FITC-toxin free in solution and AChR-bound compared to fluorescein free in solution were about what would be predicted, if the changes in translational and rotational mobility and orientation constraints are considered. These results strongly suggest that the region about lysine 23 on the receptor-bound cobra α-toxin is exposed to the bulk solvent both when the α-toxin is free in solution and when it is AChR-bound.

Tsetlin et al. (1982) attempted to determine the solute accessibility to spin-labeled N^{ϵ}-lysine 23 α-toxin (lysine 27 in their notation) bound to the *Torpedo marmorata* receptor by studying Fe^{+++} and Ni^{++}-induced paramagnetic broadening. They observed 3–5.7-fold higher apparent accessibility to the free α-toxin than to AChR-bound α-toxin. They concluded that lysine 23 is in 'contact' with the surface of the receptor. Unfortunately, because they did not measure the paramagnetic broadening of the free toxin in the presence of native α-toxin-blocked receptor, it is not possible to assess the contribution that the mere presence of the receptor may have on apparent accessibility. When we attempted to perform the analogous fluorescence quenching experiment with positively charged Tl^+ (data not shown), we observed that the quenching constant of free FITC-toxin was nearly seven times higher than AChR-bound α-toxin. However, in close agreement with our iodide experiments, the quenching constant of FITC-toxin in the presence of carbachol-blocked AChR was ~1.9 times higher than AChR-bound FITC-toxin. It is unclear why these differences occurred. Perhaps the AChR altered the chemical potential of the Tl^+ by nonspecific binding to the negatively charged surface of the AChR.

We have made many assumptions in our calculations of the bimolecular quenching rate constants. Some of these include the spherical shape, the average specific density of all the molecules involved, and the validity of the Stokes-Einstein expression for small molecules like fluorescein. So, we must stress that the predicted quenching rate constants are only first order approximations, they do show that quenching constants will decrease without an alteration of solute accessibility following binding or conjugation of a small fluorophore to a macromolecule. For the case of FITC-toxin binding to the AChR, there may be a

TABLE I
SUMMARY OF THE STERN-VOLMER QUENCHING CONSTANTS VS. DECAY RATES AND BIMOLECULAR QUENCHING RATE CONSTANTS

	K_Q	τ	$k_Q \times 10^{-9}$	Observed k_{MQ}/k_{FQ}	Theoretical k_{MQ}/k_{FQ}
	M^{-1}	*ns*	$M^{-1}s^{-1}$		
Fluorescein	9.84 ± 0.04	4.1	2.4	1.0	1.0
FITC-toxin (plus α-toxin-AChR)	4.07 ± 0.01	3.8	1.07	0.45	0.61
FITC-toxin-AChR (membrane-associated)	1.91 ± 0.01	3.9	0.48	0.20	0.38

Summary of the Stern-Volmer quenching constants (K_Q) (± standard error of estimate), the fluorescence decay rates (τ), and the bimolecular quenching rate constant (k_Q) of fluorescein, FITC-toxin free in solution (in the presence of toxin-blocked AChR) and bound to the acetylcholine receptor calculated utilizing Eq. 2. The observed k_{MQ}/k_{FQ} represents the ratio of iodide ion quenching constants for FITC-toxin and free fluorescein. The theoretical k_{MQ}/k_{FQ} indicate calculated ratio of iodide ion quenching rate constants (Eq. 6/Eq. 5) for a spherical fluorophore the size of fluorescein attached to spherical proteins the size of cobra α-toxin and the acetylcholine receptor compared relative to the rate constant for the fluorophore free in solution assuming complete accessibility ($f_{MQ} = 1$).

small change in solute accessibility to the FITC associated with AchR binding but the magnitude is probably small relative to the anticipated effect of AChR-binding.

We are unaware of any other efforts to consider rotational diffusion and orientation constraints on the fluorescence quenching technique. Failure to consider rotation and orientation constraints can potentially lead to problems in the evaluation of accessibility. Two rules of thumb appear to stem from our consideration of rotational diffusion and orientation constraints on fluorescence quenching experiments that involve comparisons between free and bound fluorophores. First, a decrease in the quenching rate constant by a factor of 2 to perhaps 5 can be expected to occur with the immobilization of a fluorophore on the surface of a macromolecule. Second, the relation between solute exposure and the quenching constant is nonlinear. The nonlinearity of this relation is particularly marked for $f_{FQ} < 0.2$, so that there is no simple direct relation between the fraction of the surface area of the fluorophore exposed to solute and the quenching rate constant (see Fig. 2 *B*).

APPENDIX

The relevant parameters for calculating k_{MQ}/k_{FQ} are evaluated as follows:

1. Translational diffusion coefficient of a spherical protein is given by the Stokes-Einstein expression

$$D_M = kT/6\pi\eta R_M(\text{cm}^2/\text{s}), \quad (13)$$

where T = 23°C, k is the Boltzmann's constant, and η is the solvent viscosity (η = 0.94 CP). Therefore,

$$D_M = 0.23 \times 10^{-4}/R_M(\text{Å})(\text{cm}^2/\text{s}). \quad (14)$$

2. The radius of a spherical protein, R_M, with molecular weight, M, is given by

$$R_M = \{(3/4\pi)[M(\upsilon + h)/N]\}^{1/3}, \quad (15)$$

where υ (cm^3/g) is the specific volume of the protein (typically 0.73 cm^3, h (cm^3/g) is the specific hydration of the typical protein (0.3 cm^3/g), and N is Avogadro's number. Using these approximate values of υ and h give

$$R_M = 0.73 \times 10^{-8}(M)^{1/3}\ (\text{cm}). \quad (16)$$

3. Rotational diffusion coefficient of a spherical protein, D_R, is given by the Stokes-Einstein expression

$$D_R = kT/6\eta V = kTN/\eta[6\pi M(\upsilon + h)] = 4.27 \times 10^{11}/M\ (\text{s}^{-1}). \quad (17)$$

4. By assuming FITC has the density of a typical protein, R_F and D_F are evaluated by substituting the molecular mass of FITC into Eqs. 16 and 14. R_F and D_F were thus estimated to be 5.3 Å and 4.3 × 10^{-6} cm^2/s, respectively. Published values of R_Q and D_Q were utilized, 2.15 Å (Gordon and Ford, 1972) and 2.04 × 10^{-5} cm^2 · s^{-1} (Erdey-Gruz, 1974), respectively.

5. The recurrence equation for the modified spherical Bessel function of the third kind of order n is given by (Abramowitz and Stegun)

$$K_{n+1}(\xi_n^*) = K_{n-1}(\xi_n^*) + (2n/\xi_n^*)K_n(\xi_n^*). \quad (18)$$

6. The recurrence relation for the nth order Legendre polynomial in $\cos\theta_o$ is given by (Abramowitz and Stegun)

$$(n + 1)P_{n+1}(\cos\theta_o) = (2n + 1)(\cos\theta_o)P_n(\cos\theta_o) - nP_{n-1}(\cos\theta_o), \quad (19)$$

where $P_{-1}(\cos\theta_o) = -1$ and $P_o(\cos\theta_o) = 1$.

7. k_{MQ}/k_{FQ} is calculated by taking the ratio of Eqs. 5 and 6. For the case where $n = 0$ Eq. 6 reduces to

$$k_{MQ} = (8\pi D_{MQ}R_{MQ}^2\kappa(1 - \cos\theta_o)^2/[(4D_{MQ}(1 - \cos\theta_o) - 2\kappa R_{MQ}^2(1 - \cos\theta_o)^2]. \quad (20)$$

(personal communication, A. Szabo).

We wish to acknowledge the technical assistance of Blake Perkins for preparation of AChR membrane fragments and the help of Drs. Keith Oddson, David Shoup, and Attila Szabo towards development of a program to solve numerically Eq. 6.

Supported in part by U.S. Public Health Service Biomedical Research Support grant RR05816, by the US Army Medical Research and Development Command, contract No. DAMD 17-84-C-4187 to D. A. Johnson, and by U.S. Public Health Service grants GM18360 and GM24437. The views, opinions and/or findings contained in this report are those of the authors and should not be construed as an official Department of the Army position, policy, or decision unless so designated by other documentation.

Received for publication 26 February 1985 and in final form 19 July 1985.

REFERENCES

Abramowitz, M., and I. A. Stegun. 1965. Handbook of Mathematical Functions with Formulas, Graphs, and Mathematical Tables. Dover Publications, Inc., New York. 1046 pp.

Cheung, A. T., D. A. Johnson, and P. Taylor, 1984. Kinetics of interaction of N^{ϵ}-fluorescein isothiocyanate-lysine-23-cobra α-toxin with the acetylcholine receptor. *Biophys. J.* 45:447–454.

Erdey-Gruz, T. 1974. Transport Phenomena in Aqueous Solutions. John Wiley & Sons, Inc., New York. 194.

Johnson, D. A., and P. Taylor. 1982. Site-specific fluorescein-labelled cobra α-toxin: biochemical and spectroscopic characterization. *J. Biol. Chem.* 257:5632–5636.

Karlsson, E., H. Arnberg, and D. Eaken. 1971. Isolation of the principal neurotoxin of two *Naja naja* subspecies. *Eur. J. Biochem.* 21:1–16.

Reed, K., P. Vandlen, J. Bode, J. Duguid, and M. A. Raftery. 1975. Characterization of acetylcholine receptor-rich and acetylcholinesterase-rich membrane particles from *Torpedo californica* electroplax. *Arch. Biochem. Biophys.* 167:138–144.

Schmidt, J., and M. A. Raftery. 1973. A simple assay for the study of solubilized acetylcholine receptors. *Anal. Biochem.* 52:349–355.

Schmitz, K. S., and J. M. Schurr. 1972. The role of orientation constraints and rotational diffusion in bimolecular solution kinetics. *J. Phys. Chem.* 76:534–545.

Schurr, J. M., and K. S. Schmitz. 1976. Orientation constraints and rotational diffusion in bimolecular solution kinetics. A simplification. *J. Phys. Chem.* 80:1934–1936.

Shoup, D., G. Lipari, and A. Szabo. 1981. Diffusion-controlled bimolecular reaction rates: The effect of rotational diffusion and orientation constraints. *Biophys. J.* 36:697–714.

Solc, K., and W. H. Stockmaker. 1971. Kinetics of diffusion-controlled reaction between chemically asymmetric molecules I. General theory. *J. Chem. Phys.* 54:2981–2988.

Solc, K., and W. H. Stockmaker. 1973. Kinetics of diffusion-controlled reaction between chemically asymmetric molecules. II. Approximate steady-state solution. *Int. J. Chem. Kinetics.* 5:733–752.

Tsetlin, V. I., E. Karlsson, Yu. N. Utkin, K. A. Pluzhnikov, A. S.

Arseniev, A. M. Surin, V. V. Kondakov, V. F. Bystrov, V. T. Ivanov, and Yu. A. Ovchinnikov. 1982. Interacting surfaces of neurotoxins and acetylcholine receptor. *Toxicon.* 20:83–93.

Weiland, G., B. Georgia, V. T. Wee, C. F. Chignell, and P. Taylor. 1976. Ligand interactions with cholinergic receptor-enriched membranes from *Torpedo:* influence of agonist exposure on receptor properties. *Mol. Pharmacol.* 12:1091–1105.

Yguerabide, J., M. A. Dillon, and M. Burton. 1964. Kinetics of diffusion-controlled processes in liquids. Theoretical consideration of luminescent systems: Quenching and excitation transfer in collision. *J. Chem. Phys.* 40:3040–3052.

Yguerabide, J. 1967. Theory of diffusion-controlled processes. II. Consideration of conceptual framework. *J. Chem. Phys.* 47:3049–3061.

Yguerabide, J. 1972. Nanosecond fluorescence spectroscopy of macromolecules. *Methods Enzymol.* 26:498–578.

Yguerabide, J., and E. E. Yguerabide. 1984. Nanosecond fluorescence spectroscopy in biological research. *In* Optical Technic. J. Doyle, editor. Academic Press Inc., New York.